Synthesis and Co-ordination Chemistry of the Pyridyl Pendant-arm Azamacrocycles 1-(2-Pyridylmethyl)-1,5,9-triazacyclododecane L^1 and 1-(2-Pyridyl-2′-ethyl)-1,5,9-triazacyclododecane L^2, with Nickel(II), Copper(II) and Zinc(II). Crystal Structures of $[Ni(L^1)(O_2NO)]NO_3$ and $[ZnL^2][Zn(NO_3)_{3.67}Cl_{0.33}]$†

Mary L. Turonek, Peter Moore,* Howard J. Clase and Nathaniel W. Alcock
Department of Chemistry, University of Warwick, Coventry CV4 7AL, UK

The azamacrocyclic ligands 1-(2-pyridylmethyl)-1,5,9-triazacyclododecane L^1 and 1-(2-pyridyl-2′-ethyl)-1,5,9-triazacyclododecane L^2 have been prepared, and their complexes with hydrated nickel(II), copper(II) and zinc(II) nitrates have been isolated. The nickel(II) complexes are high spin and six-co-ordinate, whilst ^{13}C NMR spectroscopy shows that $[ZnL^1(OH_2)]^{2+}$ exists as a symmetric trigonal-bipyramidal isomer in solution, and $[ZnL^2]^{2+}$ exists as a 2:1 mixture of tetrahedral and asymmetric trigonal-bipyramidal isomers. X-Ray crystallography has been used to determine the solid-state structures of the octahedral $[NiL^1(O_2NO)]^+$, and the tetrahedral isomer of $[ZnL^2]^{2+}$.

The stabilities of complexes formed by multidentate and macrocyclic ligands with six-co-ordinate first-row d-block transition-metal dications generally follow the Irving–Williams sequence (Mn < Fe < Co < Ni < Cu > Zn). In attempts to modify this pattern of selectivity ligands have been designed to enforce a tetrahedral geometry on a metal,[1,2] and the macrocycles described here were developed as part of ongoing studies in this area.

Previous attempts to obtain a tetrahedrally co-ordinating macrocyclic ligand have involved the development of N-monosubstituted 1,5,9-triazacyclododecane with $R_2N(CH_2)_m$ pendant arms (R = H or alkyl, $m = 2$ or 3).[1,2] The macrocycles provide a basal plane of three nitrogen donors, whilst the pendant arm supplies an apical donor. When $m = 3$, the pendant arms were found to be optimal for forming tetrahedral complexes with Zn^{II},[1] and computer modelling suggests that zinc(II) complexes have an ideal tetrahedral structure with propylene linked pendant arms which form six-membered chelate rings.[3] However, attempts to impose tetrahedral co-ordination on Cu^{II} and Ni^{II} with these ligands have been complicated by additional co-ordination of a supporting anion or solvent, thought to arise in part from the lack of steric crowding about the metal, but more importantly because of the increased crystal-field stabilisation energy (c.f.s.e.) gained by these metal ions increasing their co-ordination number from four, to five or six. Zinc(II) does not gain c.f.s.e. in this way due to its d^{10} electronic configuration, and the formation of tetrahedral structures is more favoured.

In this paper we report the synthesis of two new azamacrocyclic ligands, 1-(2-pyridylmethyl)-1,5,9-triazacyclododecane L^1 and 1-(2-pyridyl-2′-ethyl)-1,5,9-triazacyclododecane L^2, which have been synthesised using a modified Richman–Atkins method. Unlike the previous related ligand designs, the pyridyl pendant arms combine good donor strength with substantial ligand bulk, the intention being to reduce the tendency for co-ordination by the supporting anions. The nickel(II), copper(II) and zinc(II) complexes of L^1 and L^2 have been isolated, and characterised by elemental analyses, fast atom bombardment (FAB) mass spectrometry, and by proton-decoupled ^{13}C NMR for the diamagnetic zinc(II) complexes. The nickel(II) and copper(II) complexes were investigated further by UV/VIS spectroscopy and cyclic voltammetry, and the crystal and molecular structures of $[NiL^1(O_2NO)]NO_3$ and $[ZnL^2][Zn(NO_3)_{3.67}Cl_{0.33}]$ determined by X-ray crystallography.

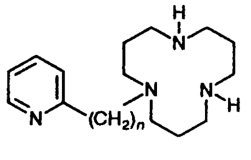

	n
L^1	1
L^2	2

Experimental

Materials.—Reagent grade commercial compounds were used as starting materials, and purity was checked by ^1H and ^{13}C NMR spectroscopy.

Spectra, Analyses and Other Procedures.—220 MHz ^1H NMR and proton-decoupled 62.9 MHz ^{13}C NMR spectra were obtained with a Bruker AC250 spectrometer and 400.13 MHz ^1H correlation spectroscopy (COSY) NMR and 100.61 MHz proton-decoupled ^{13}C NMR with a Bruker ACP400. UV/VIS and mass spectra were obtained with Shimadzu 365 and Kratos MS80 spectrometers respectively, and elemental analyses with a Leeman Laboratories CE 440 elemental analyser. Cyclic voltammetry was performed under argon at 20 °C with an Oxford electrodes potentiostat and triangular wave generator (Oxford, UK) and an Advance Bryons X–Y chart recorder. Either glassy carbon or platinum working electrodes were used, with a platinum-wire counter electrode, and a reference electrode made of a silver wire immersed in a solution of $AgNO_3$ (0.01 mol dm^{-3}) and $NaClO_4$ (0.1 mol dm^{-3})

---

† *Supplementary data available:* see Instructions for Authors, *J. Chem Soc., Dalton Trans.*, 1995, Issue 1, pp. xxv–xxx.

in acetonitrile. The supporting electrolyte was $NaClO_4$ (0.1 mol dm^{-3}), and the ferrocene–ferrocenium couple was used as an internal reference.

Preparations.—The synthetic routes are outlined in Scheme 1.

1,5-*Dicyano*-3-(2-*pyridylmethyl*)-3-*azapentane* **I**. 2-Aminomethyl pyridine (8.0 g, 0.08 mol) was dissolved in acrylonitrile (92 g, 1.72 mol), and glacial acetic acid (7.2 g, 0.16 mol) was added. Some signs of oligomerisation were evident on addition. The resulting slurry was stirred with a magnetic follower and heated at reflux under dry N_2 for 24 h, after which the solid dissolved and the solution changed to deep yellow. Excess acrylonitrile was removed with a rotary evaporator under reduced pressure, and dichloromethane (150 cm^3) was added to the remaining residue. The organic solution was washed with 0.88 NH_3 solution (125 cm^3), distilled water (3 × 100 cm^3) and then dried with anhydrous Na_2SO_4. After filtration, the solvent was removed to give the product as a yellow oil (11.18 g, 52 mmol, 65% yield). NMR ($CDCl_3$): ^1H, δ 8.48 (1 H, d), 7.66 (1 H, t), 7.49 (1 H, d), 7.19 (1 H, t), 3.84 (2 H, s), 2.92 (4 H, t) and 2.48 (4 H, t); ^{13}C (abundances 1 unless specified), δ 157.6, 148.6, 136.5, 122.7, 122.1, 118.3, 59.0, 49.1 (2) and 16.3 (2). Electron impact mass spectrum: *m/z* 214 (calc. for M^+ 214).

5-(2-*Pyridylmethyl*)-1,5,9-*triazanonane* **II**. To a 50% suspension of active Raney nickel (8.1 g) in water (*ca.* 10 cm^3) was added a solution of **I** (11.18 g, 0.052 mol) in methanol (225 cm^3). The solution was vigorously stirred, and a solution of $NaBH_4$ (4.04 g, 0.106 mol) in 8 mol dm^{-3} NaOH (57 cm^3) was added at such a rate as to maintain the temperature at 60 °C. After addition was complete, the reaction mixture was stirred at room temperature overnight. The Raney nickel catalyst was then removed by filtration through Celite, and the solvent was removed under reduced pressure. A portion of 8 mol dm^{-3} NaOH (57 cm^3) was added to the residue, which was then extracted with dichloromethane (5 × 50 cm^3). The organic washings were combined, dried with anhydrous Na_2SO_4, and after filtration the solvent was removed to give the product as a yellow oil (7.98 g, 36 mmol, 69% yield). NMR ($CDCl_3$): ^1H, δ 8.00 (1 H, d), 7.15 (1 H, t), 6.96 (1 H, d), 6.63 (1 H, t), 3.21 (2 H, s), 2.20 (4 H, t), 2.03 (4 H, t), 1.13 (4 H, q) and 1.05 (4 H, br s); ^{13}C, δ 159.4, 147.8, 135.3, 121.8, 120.8, 59.6, 50.9 (2), 39.4 (2) and 29.9 (2). Electron impact mass spectrum: *m/z* 222 (calc. for M^+ 222).

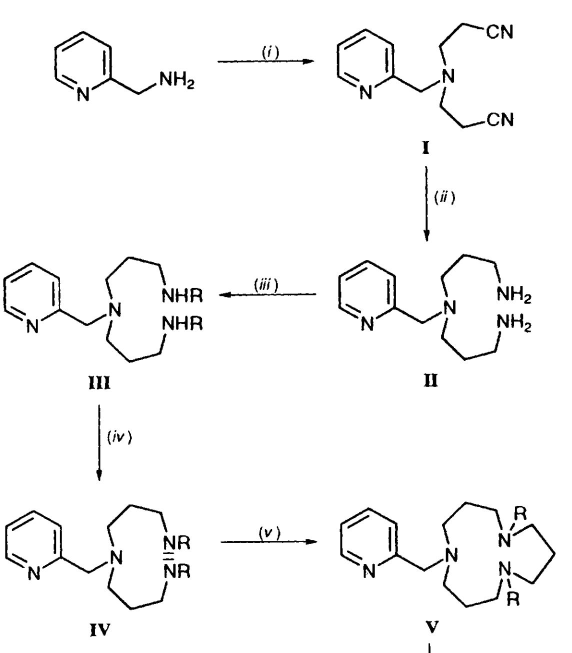

Scheme 1 R = p-$MeC_6H_4SO_2$ (*i*) acrylonitrile, acetic acid; (*ii*) Raney Ni, $NaBH_4$, OH^-; (*iii*) p-$MeC_6H_4SO_2Cl$; (*iv*) Na, EtOH; (*v*) $Br(CH_2)_3Br$, dmf; (*vi*) concentrated H_2SO_4; (*vii*) OH^-

1,9-*Bis*(*toluene*-p-*sulfonyl*)-5-(2-*pyridylmethyl*)-1,5,9-*triazanonane* **III**. A solution of toluene-*p*-sulfonyl chloride (13.73 g, 0.072 mol) in diethyl ether (72 cm^3) was added dropwise at room temperature to a vigorously stirred solution of **II** (7.98 g, 0.036 mol) and NaOH (2.88 g, 0.072 mol) in water (24 cm^3). When the addition was complete, the solution was stirred overnight, to give a thick yellow oil which separated and was isolated by decanting off the aqueous and organic layers. The oil was dissolved in dichloromethane (75 cm^3) and the aqueous layer was washed with dichloromethane (3 × 50 cm^3). These washings were combined with the other dichloromethane fraction and dried with anhydrous Na_2SO_4. After filtration, the solvent was removed to give the product as a thick toffee-like yellow oil (11.56 g, 22 mmol, 61% yield). NMR ($CDCl_3$): ^1H, δ 8.68 (1 H, d), 7.60 (1 H, t), 7.59 (4 H, d), 7.15 (4 H, d), 7.14 (1 H, d), 6.96 (1 H, t), 3.55 (2 H, s), 2.86 (4 H, t), 2.38 (4 H, t), 2.30 (6 H, s) and 1.52 (4 H, q); ^{13}C, δ 157.3, 149.5, 142.7 (2), 137.3 (2), 136.8, 129.4 (4), 126.7 (4), 123.0, 122.4, 58.1, 51.5 (2), 41.4 (2), 25.4 (2) and 21.2 (2). Electron impact mass spectrum: *m/z* 531 (calc. for M^+ 531).

Disodium salt of **III** (**IV**). Compound **III** was dissolved in absolute ethanol (100 cm^3) and added dropwise to a stirred solution of sodium (2 g) in absolute ethanol (100 cm^3) under an N_2 atmosphere. After stirring for 1 h, the solvent was removed under reduced pressure to yield **IV** as a thick toffee-like product (12.6 g, 22 mmol, 100% yield).

1-(2-*Pyridylmethyl*)-5,9-*bis*(*toluene*-p-*sulfonyl*)-1,5,9-*triazacyclododecane* **V**. A solution of 1,3-dibromopropane (7.27 g, 0.036 mol) in anhydrous dimethyl formamide (136 cm^3) was added dropwise to a stirred solution of the disodium salt **IV** in anhydrous dimethyl formamide (272 cm^3) kept at 110 °C under an N_2 atmosphere. When the addition was complete (2 h), the solution was cooled and water was added dropwise with stirring until the volume reached 1.25 dm^3. The solution was further stirred for 8 h, and an oily residue settled on the sides of the flask. The solution was then evaporated under reduced pressure, and the oily residue was redissolved in dimethyl formamide. A cream-white precipitate settled out of solution. This was collected by vacuum filtration, then washed with ethanol (2 × 100 cm^3) and diethyl ether (100 cm^3) (7.65 g, 13.4 mmol, 61% yield). NMR ($CDCl_3$): ^1H, δ 8.44 (1 H, d), 7.60 (1 H, t, 4 H, d), 7.27 (4 H, d, 1 H, d), 7.12 (1 H, t), 3.55 (2 H, s), 2.86 (4 H, t), 2.38 (4 H, t), 2.30 (6 H, s) and 1.52 (4 H, q); ^{13}C, δ 159.1, 148.9, 143.3 (2), 136.4, 135.2 (2), 129.6 (4), 127.2 (4), 123.1, 122.0, 60.0, 50.0 (2), 45.5 (2), 44.5 (2), 24.8, 24.0 (2) and 21.4 (2). Electron impact mass spectrum: *m/z* 571 (calc. for M^+ 571).

1-(2-*Pyridylmethyl*)-1,5,9-*triazacyclododecane* (**VI**; L^1). To remove the toluene-*p*-sulfonyl functional groups from **V**, 7.6 g of **V** were dissolved in a stirred solution of N_2-scrubbed concentrated sulfuric acid (70 cm^3) at 100 °C, and the hot mixture stirred for 2 days. After cooling on ice, diethyl ether (170 cm^3) was added to the black solution containing the acid and the tosylated starting material. The diethyl ether–acid solution was decanted from the resulting sticky precipitate, which was then dissolved in water (30 cm^3). Sodium hydroxide solution (8 mol dm^{-3}) was added dropwise to increase the pH to > 12. The aqueous solution was then extracted with dichloromethane (5 × 50 cm^3), the combined extracts dried with anhydrous Na_2SO_4, filtered, and the solvent was removed under reduced pressure to leave a yellow oil (1.74 g, 6.6 mmol, 49% yield). NMR ($CDCl_3$): ^1H, δ 8.32 (1 H, d), 7.46 (1 H, t), 7.22

(1 H, d), 6.94 (1 H, t), 3.44 (2 H, s), 2.66 (4 H, t), 2.50 (4 H, t), 2.38 (4 H, t) and 1.54 (6 H, m); ^{13}C, δ 159.1, 148.6, 135.9, 122.7, 121.5, 58.4, 52.4 (2), 48.8 (2), 46.4 (2), 25.2 and 24.9 (2). Electron impact mass spectrum: *m*/*z* 262 (calc. for M^+ 262).

1-(*2-Pyridyl-2′-ethyl*)-1,5,9-*triazacyclododecane* (L^2). Compound L^2 and its synthetic precursors were prepared in an analogous fashion to L^1 using the starting material 2-(2-aminoethyl)pyridine. The results are summarised below.

1,5-*Dicyano*-3-(2-*pyridyl-2′-ethyl*)-3-*azapentane* **VII**. The product was obtained as a yellow oil (15.9 g, 70 mmol, 87% yield). NMR ($CDCl_3$): ^{1}H, δ 8.33 (1 H, d), 7.42 (1 H, t), 7.00 (1 H, d), 6.94 (1 H, t), 2.77 (4 H, m), 2.68 (4 H, t) and 2.24 (4 H, t); ^{13}C, δ 158.9, 148.6, 135.9, 123.1, 120.9, 118.3, 52.5, 49.0 (2), 35.6 and 16.4 (2). Electron impact mass spectrum: *m*/*z* 228 (calc. for M^+ 228).

5-(*2-Pyridyl-2′-ethyl*)-*1,5,9-triazanonane* **VIII**. The product was a yellow oil (8.2 g, 35 mmol, 50% yield). NMR ($CDCl_3$): ^{1}H, 8.33 (1 H, d), 7.40 (1 H, t), 6.98 (1 H, d), 6.91 (1 H, t), 2.41 (4 H, m), 2.19 (4 H, t), 2.06 (4 H, t), 1.11 (4 H, q) and 1.07 (4 H, br s); ^{13}C, 160.4, 148.8, 135.8, 122.9, 120.7, 53.7 (2), 51.4 (2), 40.2 (2), 35.4 and 30.7. Electron impact mass spectrum: *m*/*z* 237 (calc. for M^+ 237).

1,9-*Bis*(*toluene*-p-*sulfonyl*)-5-(*2-pyridyl-2′-ethyl*)-1,5,9-*triazanonane* **IX**. The product was obtained as a thick toffee-like yellow oil (18.7 g, 34 mmol, 98% yield). NMR ($CDCl_3$): ^{1}H, δ 8.36 (1 H, d), 7.64 (4 H, d), 7.50 (1 H, t), 7.29 (4 H, d), 7.07 (1 H, d), 7.02 (1 H, t), 2.80 (8 H, m), 2.50 (4 H, t), 2.31 (6 H, s) and 1.55 (4 H, q); ^{13}C, δ 159.4, 148.6, 142.8 (2), 136.9 (2), 136.5, 129.4 (4), 126.8 (4), 123.2, 121.3, 53.4 (2), 51.2 (2), 41.4 (2), 34.1, 25.5 and 21.2 (2). Electron impact mass spectrum: *m*/*z* 544 (calc. for M^+ 544).

Disodium salt of **IX** (**X**). A quantitative yield of a thick toffee-like substance was obtained (20 g, 34 mmol).

1-(*2-Pyridyl-2′-ethyl*)-5,9-*bis*(*toluene*-p-*sulfonyl*)-1,5,9-*triazacyclododecane*. The product was obtained as a cream-white precipitate (3.14 g, 5.4 mmol, 16% yield). NMR ($CDCl_3$): ^{1}H, δ 8.43 (1 H, d), 7.63 (4 H, d), 7.49 (1 H, t), 7.29 (4 H, d), 7.07 (1 H, d), 7.02 (1 H, t), 3.07 (4 H, t), 2.96 (4 H, t), 2.79 (4 H, m), 2.45 (4 H, t), 2.42 (6 H, s), 1.68 (4 H, q) and 1.54 (2 H, q); ^{13}C, δ 160.7, 149.2, 143.2 (2), 136.1, 135.3 (2), 129.6 (4), 127.2 (4), 123.4, 121.0, 52.3, 49.7 (2), 45.4 (2), 44.0 (2), 34.6, 24.1 (2), 23.6 and 21.4 (2). Electron impact mass spectrum: *m*/*z* 587 (calc. for M^+ 587).

1-(*2-Pyridyl-2′-ethyl*)-1,5,9-*triazacyclododecane* (**XII**; L^2). The product was a yellow oil (0.74 g, 2.7 mmol, 49% yield). NMR ($CDCl_3$): ^{1}H, δ 8.33 (1 H, d), 7.40 (1 H, t), 6.99 (1 H, d), 6.92 (1 H, t), 2.74 (2 H, t), 2.62 (2 H, t), 2.52 (4 H, t), 2.44 (8 H, m), 1.50 (4 H, q) and 1.39 (2 H, q); ^{13}C, 160.4, 148.8, 135.8, 123.0, 120.6, 51.9 (2), 51.6, 49.0 (2), 46.3 (2), 33.8, 25.2 (2) and 24.8. Electron impact mass spectrum: *m*/*z* 276 (calc. for M^+ 276).

Metal complexes of L^1 *and* L^2. These were obtained in *ca.* 50–70% yields by adding a solution of the appropriate hexaaqua solvates of the metal nitrates (0.5 mmol) in *n*-butanol (10 cm^3) to an equimolar amount of each ligand in *n*-butanol (5 cm^3). The mixtures were stirred for 1 h, whereupon the solid products separated. These were collected by filtration, and crystals suitable for X-ray analysis grown from slow diffusion of diethyl ether into a saturated nitromethane–ethanol solution. The products were finally washed with ethanol and diethyl ether. The elemental analyses are collected in Table 1, proton-decoupled ^{13}C NMR chemical shifts of the diamagnetic zinc(II) complexes are compared with those of the free ligands in Table 2, and details of the visible spectra of the nickel(II) and copper(II) complexes are collected in Table 3. The cyclic voltammetry data are in Table 4.

Crystal Structure Analysis of $[NiL^1(O_2NO)]NO_3$ *and* $[ZnL^2][Zn(NO_3)_{3.67}Cl_{0.33}]$.—Crystals of $C_{15}H_{26}N_6NiO_6$ and $C_{16}H_{28}Cl_{0.33}N_{7.67}O_{11.01}Zn_2$ suitable for crystallography were obtained as deep purple well formed blocks, and small colourless prisms respectively. Crystal data for the complexes are given in Table 5 together with details of the data collection and structure determination. Data were collected with a Siemens R3m four-circle diffractometer in ω–2θ mode using graphite-monochromated Mo-Kα radiation. The crystals were held at 200 and 220 K respectively, using an Oxford Cryosystems Cryostream cooler.[5] Scan range was ±0.75°(ω) around the $K\alpha_1$–$K\alpha_2$ angles, scan speed 1.5°(ω) min^{-1}, depending on the intensity of a 2 s pre-scan; backgrounds were measured at each end of the scan for 0.25 of the scan time. Three standard reflections were monitored every 200, and showed a slight decrease, and a 9% decrease, during data collection for the nickel(II) and zinc(II) complexes respectively. The data were rescaled to correct for this. Unit-cell dimensions and standard deviations were obtained by least-squares fit to 15 high-angle reflections. Reflections were processed using profile analysis, and were corrected for Lorentz, polarisation and in the case of the nickel complex for absorption effects by the analytical method using ABSPSI.[6] Systematic reflection conditions indicated the space groups unambiguously. Heavy atoms were located by the Patterson interpretation section of SHELXTL PLUS,[7] and the light atoms then found by E-map expansion and successive Fourier syntheses. A partially occupied disordered solvent molecule was located for the nickel(II) complex. This was modelled by four C atoms of occupancy 0.3 adjacent to a centre of inversion. The E-map expansion and successive Fourier syntheses of the zinc(II) complex showed the unexpected presence of $[Zn(NO_3)_4]^{2-}$. The nitrogen of one NO_3^- group [N(60)] showed anomalously low thermal parameters, while its oxygens had relatively high values. This was identified as due to partial substitution (33%) of Cl^- for the NO_3^-. This NO_3^- was constrained to be flat. Atom C(7) in this complex has two alternative (50%) positions. Anisotropic displacement parameters were used for all non-H atoms (apart from the solvent molecule in the Ni complex). Hydrogen atoms were given fixed isotropic displacement parameters, $U = 0.08$ Å^2. Those defined by the molecular geometry were inserted at calculated positions and not refined. For the zinc(II) complex the absolute structure of the individual crystal chosen was checked by refinement of a $\delta f''$ multiplier. Final refinement was on F^2 by least-squares methods. A weighting scheme was used of the form $w = 1/[\sigma^2(F_o^2) + (aP)^2 + bP]$, where $P = (F_o^2 + 2F_c^2)/3$, with $a = 1.097$, $b = 3.5678$ for $C_{15}H_{26}N_6NiO_6$, and $a = 0.1311$, $b = 6.0549$ for $C_{16}H_{28}Cl_{0.33}N_{7.67}O_{11.01}Zn_2$; this was shown to be satisfactory

Table 1 Elemental analyses (%, calculated values in parentheses), colours and proposed formulations of metal complexes of L^1 and L^2

Complex	Colour	C	H	N
$[CuL^1(ONO_2)][CuL^1(OH)][Cu(NO_3)_4]\cdot 2H_2O$	Blue	33.4 (33.4)	5.5 (5.3)	16.1 (16.8)
$[NiL^1(O_2NO)]NO_3\cdot EtOH$	Purple	41.8 (41.6)	6.4 (6.6)	17.0 (17.1)
$[ZnL^1(ONO_2)][ZnL^1(OH)][Zn(NO_3)_4]\cdot H_2O$	White	33.5 (33.8)	4.9 (5.2)	16.8 (17.1)
$[CuL^2][NO_3]_2\cdot 0.5H_2O$	Blue	40.7 (40.6)	6.0 (6.2)	17.2 (17.7)
$[NiL^2(O_2NO)]NO_3\cdot H_2O$	Lavender	40.7 (40.3)	6.4 (6.3)	17.0 (17.6)
$[ZnL^2][Zn(NO_3)_4]$ *	White	29.7 (29.3)	4.4 (4.3)	16.6 (17.1)

* Adventitious chloride was introduced during crystal growth to give a complex of formula $[ZnL^2][Zn(NO_3)_{3.67}Cl_{0.33}]$.

Table 2 Carbon-13 NMR chemical shifts δ (reference $SiMe_4$) at 298K in $CDCl_3$ for L^1 and L^2, and for their zinc(II) complexes in CD_3CN solution (relative populations in parentheses)

Assignment	L^1	$[ZnL^1]^{2+a}$	L^2	$[ZnL^2]^{2+a}$	$[ZnL^2]^{2+b}$
pyridyl (pyr)	159.1(1)	156.0(1)	160.4(1)	161.7(1)	162.1(1)
	148.6(1)	148.6(1)	148.8(1)	150.2(1)	150.2(1)
	135.9(1)	141.9(1)	135.8(1)	142.4(1)	141.2(1)
	122.7(1)	125.8(1)	123.0(1)	126.9(1)	125.9(1)
	121.5(1)	125.4(1)	120.6(1)	124.5(1)	123.8(1)
pyr-CH_2N	58.4(1)	61.3(1)			
pyr-$\mathit{C}H\mathit{C}H_2$			51.6(1)	56.5(1)	62.3, 59.0(1)
			33.8(1)	32.6(1)	31.6, 25.7(1)
$N\mathit{C}H_2C$	52.4(2)	59.1(2)	51.9(2)	57.9(2)	57.2, 55.5(2)
	48.8(2)	52.2(2)	49.0(2)	51.0(2)	50.9, 50.2(2)
	46.4(2)	52.1(2)	46.3(2)	50.4(2)	49.3, 47.1(2)
$C\mathit{C}H_2C$	25.2(1)	25.6(1)	25.2(2)	27.0(1)	25.3, 24.4(2)
	24.9(2)	24.7(2)	24.8(1)	23.5(2)	19.7, 14.2(1)

[a] Symmetric isomer. [b] Asymmetric isomer.

Table 3 UV/VIS spectra of the complexes of Cu^{II} and Ni^{II} with L^1 and L^2 in acetonitrile at 298 K

Complex	Colour	λ_{max}/nm (ε/dm^3 mol^{-1} cm^{-1})
$[CuL^1(ONO_2)][CuL^1(OH)][Cu(NO_3)_4]\cdot 2H_2O$	Blue	675 (330), 450 (25.6)
$[NiL^1(O_2NO)]NO_3\cdot EtOH$	Lavender	860 (10.6), 540 (24.6)
$[CuL^2][NO_3]_2\cdot 0.5H_2O$	Blue	654 (184)
$[NiL^2(O_2NO)]NO_3\cdot H_2O$	Lavender	862 (14.4), 554 (40)

Table 4 Anode peak potentials (E_{pa}/V *versus* NHE) unless specified otherwise (NHE = natural hydrogen electrode)

Species	Redox couple	Glassy carbon electrode	Platinum electrode
$[CuL^2]^{2+}$	Cu^{III}–Cu^{II}	2.03	1.91
$[CuL^3]^{2+a}$	Cu^{II}–Cu^{Ib}	$-0.21^{c,d}$	
$[NiL^1]^{2+}$	Ni^{III}–Ni^{IIe}	1.73	1.97
$[NiL^2]^{2+}$	Ni^{III}–Ni^{IIe}	1.55	1.60
$[NiL^3]^{2+}$	Ni^{III}–Ni^{IIe}	> 1.9	

[a] L^3 = 1,5,9-Tris(2-pyridylmethyl)-1,5,9-triazacyclododecane. [b] Reversible redox couple. [c] $E_{\frac{1}{2}}$, the redox potential for a reversible couple, calculated from $E_{\frac{1}{2}} = (E_{pa} + E_{pc})/2$. [d] Ref. 4. [e] Irreversible redox couple.

by a weight analysis. The maximum shift/error for the nickel and zinc crystals were 0.05 and 0.003, respectively. Computing was with SHELXTL PLUS[7] on a DEC Microvax-II, with final refinement by SHELXL[8] on a Sun UNIX system. Scattering factors in the analytical form and anomalous dispersion factors were taken from International Tables (1974; stored in the program).[9] Final atomic coordinates for $[NiL^1(O_2NO)]NO_3$ are given in Table 6, and selected bond lengths and angles in Table 7. Final atomic coordinates for $[ZnL^2][Zn(NO_3)_{3.67}Cl_{0.33}]$ are given in Table 8, and selected bond lengths and angles are in Table 9.

Additional data available from the Cambridge Crystallographic Data Centre comprises H-atom coordinates, thermal parameters and remaining bond lengths and angles.

Results and Discussion

Ligand Syntheses.—There are several ways to approach the monoalkylation of triazamacrocycles. To add a single pendant arm, the simplest approach is to attach it to one of the secondary amines of a previously prepared triazamacrocycle, by nucleophilic attack by an amino group at an alkyl halide (or a compound containing some other leaving group) in the presence of a proton scavenger. This technique has been adopted successfully, especially in the case of triazacyclononane.[3,10,11] However, the disadvantage of this approach lies in the formation of mixtures of mono-, di- and tri-substituted species, and the consequent difficulty in separating these products. Controlled monoalkylation is often difficult because of the pH sensitivity of the reaction. The pK_a of triazamacrocycles of different ring sizes may vary as much as two orders of magnitude because of strong intramolecular hydrogen bonding within the ring.[12–15] Raising the pH of the reaction mixture to overcome the resistance of the macrocycle to nucleophilic addition also promotes some side reactions in addition to the formation of the desired ligand.[16] The second approach is a more recent development which is gaining favour, and which allows controlled stepwise addition of pendant arms to the macrocycle. Here, the approach is to attach the pendant arm to the macrocycle *via* a 'capped' macrocycle or tricyclic orthoamide, and subsequently react the orthoamide functional group with the halogenated pendant arm. Acid hydrolysis affords the formyl derivative which can then undergo base hydrolysis to give the desired ligand.[4,17,18] The synthesis of L^1 may be achieved using this approach, starting with 1,5,9-triazacyclododecane followed by the reaction of the orthoamide with 2-(chloromethyl)pyridine. However, the analogue of 2-(chloromethyl)pyridine required for the synthesis of L^2 is not readily available. The third approach, which was used in this work (Scheme 1), is to construct the macrocycle starting with the pre-formed pendant arm. The starting material is a pendant arm which terminates in a primary amino functional group. This is reacted in glacial acetic acid with acrylonitrile to add two 2-cyanoethyl groups. The cyano functionalities are successfully reduced to primary amines by reaction with Raney nickel and sodium tetrahydridoborate under alkaline conditions, without reduction of the aromatic ring of the pendant arm. The remaining cyclisation reaction follows a modified Richman–Atkins method. This approach produces the ligands L^1 and L^2 in moderate yield. The ligands are characterised by their ^1H and ^{13}C NMR spectra (Table 2), and their mass spectra, and by the analytical data for their metal complexes (Table 1).

Metal Complexes of L^1 *and* L^2.—These are obtained from mixing equimolar amounts of the appropriate ligand and the hydrated metal(II) nitrate salts in *n*-butanol. In general, the metal complexes of L^2 are more difficult to handle than those of L^1, since they are more hygroscopic, and often decompose upon filtration from the mother-liquor. This suggests a lower stability

Table 5 Crystallographic data for $[NiL^1(O_2NO)]NO_3$ and $[ZnL^2][Zn(NO_3)_{3.67}Cl_{0.33}]$

Compound	$[NiL^1(O_2NO)]NO_3$	$[ZnL^2][Zn(NO_3)_{3.67}Cl_{0.33}]$
Formula	$C_{15}H_{26}N_6NiO_6$	$C_{16}H_{28}Cl_{0.33}N_{7.67}O_{11.01}Zn_2$
M_r	445.13	646.24
Crystal system	Monoclinic	Orthorhombic
a/Å	11.292(7)	9.353(10)
b/Å	13.000(11)	14.98(2)
c/Å	16.22(2)	17.529(12)
β/°	109.75(7)	90
U/Å^3	2241(3)	2456(4)
T/K	200(2)	220(2)
Space group	$P2_1/c$	$P2_12_12_1$
Systematic absences	$h0l, l \neq 2n; 0k0, k \neq 2n$	$h00, h \neq 2n; 0k0, k \neq 2n; 00l, l \neq 2n$
Z	4	4
D_c/g cm^{-3}	1.320	1.748
Colour, habit	Deep purple well-formed blocks	Colourless prisms
Crystal size/mm	0.66 × 0.60 × 0.43	0.40 × 0.35 × 0.30
μ/mm^{-1}	0.905	2.062
F(000)	936	1325
$\theta_{min}, \theta_{max}$/°	1.5, 25	1.5, 25
Index ranges	0–13, 0–15, −19 to 18	0–11, −1 to 17, −1 to 20
Number of data collected	4051	5100
Independent reflections	3844	4352
Absorption correction	Analytical	None
Max., min transmission	0.76, 0.57	
$R(F)$ [$I > 2\sigma(I)$]	0.0511	0.0605
wR (F^2) (all data)	0.1759	0.1867
Goodness of fit on F^2	1.059	1.040
Largest difference peak, hole/e Å^{-3}	0.737, −0.912	0.640, −1.059
Data, restraints, parameters	3833, 0, 269	4348, 1, 353

Table 6 Atomic coordinates (× 10^4) for $[NiL^1(O_2NO)]NO_3$

Atom	x	y	z
Ni	7 313.4(4)	−235.7(3)	8 282.8(3)
N(01)	8 928(3)	−1 574(3)	8 206(2)
O(11)	9 264(3)	−695(2)	8 538(2)
O(12)	7 772(3)	−1 719(2)	7 832(2)
O(13)	9 687(4)	−2 257(3)	8 248(3)
N(1)	7 614(3)	1 100(2)	9 015(2)
C(2)	6 467(3)	1 754(3)	8 754(2)
C(3)	5 265(4)	1 165(3)	8 684(2)
C(4)	4 692(3)	578(3)	7 824(2)
N(5)	5 401(3)	−366(2)	7 796(2)
C(6)	4 987(4)	−856(3)	6 915(3)
C(7)	5 320(4)	−273(3)	6 208(3)
C(8)	6 708(4)	−48(3)	6 387(2)
N(9)	7 193(3)	606(2)	7 173(2)
C(10)	8 362(4)	1 165(3)	7 282(3)
C(11)	8 549(4)	2 010(3)	7 963(3)
C(12)	8 690(4)	1 673(3)	8 893(3)
C(13)	7 970(4)	837(3)	9 967(2)
C(14)	7 779(4)	−274(3)	10 141(3)
N(15)	7 504(3)	−925(2)	9 468(2)
C(16)	7 357(4)	−1 931(3)	9 612(3)
C(17)	7 508(5)	−2 306(4)	10 432(3)
C(18)	7 805(4)	−1 630(4)	11 133(3)
C(19)	7 943(4)	−598(4)	10 988(3)
N(02)	5 712(3)	2 188(2)	1 020(2)
O(21)	5 403(3)	2 504(2)	1 643(2)
O(22)	5 734(4)	1 248(2)	891(2)
O(23)	5 976(4)	2 801(3)	529(2)
C(001)	1 386(30)	351(23)	6 119(20)
C(002)	972(22)	−3(18)	6 246(15)
C(003)	44(23)	228(17)	5 363(15)
C(004)	1 271(15)	598(12)	6 781(10)

Table 7 Selected bond lengths (Å) for $[NiL^1(O_2NO)]NO_3$

Ni–N(5)	2.040(3)	Ni–N(15)	2.065(4)
Ni–N(1)	2.065(3)	Ni–N(9)	2.071(3)
Ni–O(11)	2.182(3)	Ni–O(12)	2.186(3)
N(01)–O(13)	1.220(5)	N(01)–O(12)	1.254(5)
N(01)–O(11)	1.266(5)	N(1)–C(2)	1.487(4)
N(1)–C(12)	1.495(5)	N(1)–C(13)	1.498(5)
C(2)–C(3)	1.529(5)	C(3)–C(4)	1.524(6)
C(4)–N(5)	1.476(5)	N(5)–C(6)	1.489(5)
C(6)–C(7)	1.523(6)	C(7)–C(8)	1.523(6)
C(8)–N(9)	1.476(5)	N(9)–C(10)	1.465(5)
C(10)–C(11)	1.521(6)	C(11)–C(12)	1.527(6)
C(13)–C(14)	1.501(6)	C(14)–N(15)	1.333(5)
C(14)–C(19)	1.387(6)	N(15)–C(16)	1.349(5)
C(16)–C(17)	1.371(6)	C(17)–C(18)	1.385(8)
C(18)–C(19)	1.381(7)	N(02)–O(23)	1.232(4)
N(02)–O(22)	1.242(5)	N(02)–O(21)	1.245(4)
C(001)–C(002)	0.73(3)	C(001)–C(004)	1.17(3)
C(001)–C(003)	1.60(4)	C(002)–C(004)	1.13(3)
C(002)–C(003)	1.49(3)	C(003)–C(003′)	1.29(4)

than the complexes of L^1, and may be a result of a lower co-ordination number at the metal ion, and steric crowding within the metal complex.[1] The UV/VIS spectrum of each species is consistent with the formulations given in Table 1. The pale lavender solutions of the nickel(II) complexes have UV/VIS spectra that are characteristic of six-co-ordinate high-spin d^8 ions (Table 3). The UV/VIS spectra of both copper(II) complexes show a broad d–d band in the visible region, and do not allow a distinction between either five- or six-co-ordination. With the exception of $[ZnL^2]^{2+}$, the presence of co-ordinated water molecules in each species is confirmed by the presence of a broad O–H band in the infrared spectra at 3000 cm^{-1}.

Cyclic voltammograms of millimolar solutions of the copper(II) and nickel(II) complexes in acetonitrile solution were run in the scan range −1.4 to +2.0 V (*versus* Ag–Ag$^+$), giving the redox potentials collected in Table 4. No redox couple was observed for $[CuL^1]^{2+}$ using either glassy carbon or platinum working electrodes. An irreversible anodic peak was observed for oxidation of $[CuL^2]^{2+}$ to Cu^{III}, but cathodic peaks corresponding to the reduction to Cu^I was not observed for either of the copper(II) complexes. This behaviour contrasts with that reported for $[CuL^3]^{2+}$ [L^3 = 1,5,9-tris(2-pyridylmethyl)-1,5,9-triazacyclododecane], for which a reversible reduction to Cu^I, but no oxidation to Cu^{III} was observed.[4]

Table 8 Atomic coordinates (× 10^4) for $[ZnL^2][Zn(NO_3)_{3.67}Cl_{0.33}]$

Atom	x	y	z
Zn(1)	7 558.8(8)	8 185.9(5)	7 821.7(4)
N(1)	9 528(7)	8 361(5)	7 348(4)
C(2)	9 930(10)	9 322(6)	7 324(5)
C(3)	8 676(13)	9 940(6)	7 188(6)
C(4)	7 786(13)	10 137(6)	7 858(5)
N(5)	6 790(8)	9 400(4)	8 062(4)
C(6)	6 256(11)	9 487(6)	8 864(5)
C(7A)	7 229(13)	9 043(8)	9 446(6)
C(7B)	5 915(48)	8 686(29)	9 209(25)
C(8)	7 204(11)	8 076(7)	9 479(5)
N(9)	7 833(7)	7 566(4)	8 823(4)
C(10)	9 325(10)	7 298(7)	8 970(6)
C(11)	10 455(10)	7 926(8)	8 655(6)
C(12)	10 642(8)	7 873(7)	7 798(6)
C(13)	9 504(10)	8 009(6)	6 553(5)
C(14)	8 736(10)	7 123(6)	6 468(5)
C(15)	7 146(9)	7 203(5)	6 404(4)
C(16)	6 404(11)	6 867(6)	5 783(5)
C(17)	4 940(11)	6 946(6)	5 754(5)
C(18)	4 249(10)	7 363(6)	6 341(5)
C(19)	5 014(9)	7 691(6)	6 936(5)
N(20)	6 443(7)	7 608(4)	6 980(3)
Zn(2)	14 369.1(11)	10 173.4(7)	5 921.1(6)
N(30)	11 753(9)	9 974(5)	5 488(4)
O(31)	12 448(8)	9 339(4)	5 785(4)
O(32)	12 423(11)	10 664(4)	5 350(4)
O(33)	10 474(8)	9 874(6)	5 360(4)
N(40)	15 978(7)	9 175(4)	5 069(4)
O(41)	15 037(8)	9 626(6)	4 740(4)
O(42)	16 035(8)	9 260(5)	5 774(4)
O(43)	16 746(9)	8 680(5)	4 698(5)
N(50)	13 310(7)	10 246(5)	7 419(4)
O(51)	14 343(7)	9 870(5)	7 046(3)
O(52)	12 552(7)	10 783(4)	7 084(3)
O(53)	13 136(9)	10 048(6)	8 076(4)
N(60)	15 913(27)	11 704(17)	6 210(14)
O(61)	14 861(11)	11 425(6)	5 822(6)
O(62)	15 971(13)	12 522(7)	6 319(7)
O(63)	16 795(16)	11 238(9)	6 440(10)
Cl(1)	15 711(19)	11 545(10)	6 218(9)

Table 9 Selected bond lengths (Å) and angles (°) for $[ZnL^2][Zn(NO_3)_{3.67}Cl_{0.33}]$

Zn(1)–N(5)	2.001(7)	Zn(1)–N(9)	2.002(6)
Zn(1)–N(20)	2.004(6)	Zn(1)–N(1)	2.037(6)
N(1)–C(2)	1.489(11)	N(1)–C(13)	1.490(11)
N(1)–O(12)	1.497(10)	C(2)–C(3)	1.51(2)
C(3)–C(4)	1.47(2)	C(4)–N(5)	1.487(12)
N(5)–C(6)	1.497(12)	C(6)–C(7B)	1.38(4)
C(6)–C(7A)	1.520(14)	C(7A)–C(8)	1.45(2)
C(7B)–C(8)	1.59(4)	C(8)–N(9)	1.501(11)
N(9)–C(10)	1.474(11)	C(10)–C(11)	1.52(2)
C(11)–C(12)	1.514(14)	C(13)–C(14)	1.516(13)
C(14)–C(15)	1.496(13)	C(15)–N(20)	1.349(10)
C(15)–C(16)	1.385(12)	C(16)–C(17)	1.375(14)
C(17)–C(18)	1.365(14)	C(18)–C(19)	1.357(12)
C(19)–N(20)	1.344(10)		
N(5)–Zn(1)–N(9)	106.4(3)	N(5)–Zn(1)–N(20)	111.1(3)
N(9)–Zn(1)–N(20)	120.8(3)	N(5)–Zn(1)–N(1)	107.1(3)
N(1)–Zn(1)–N(9)	107.5(3)	N(20)–Zn(1)–N(1)	103.1(3)

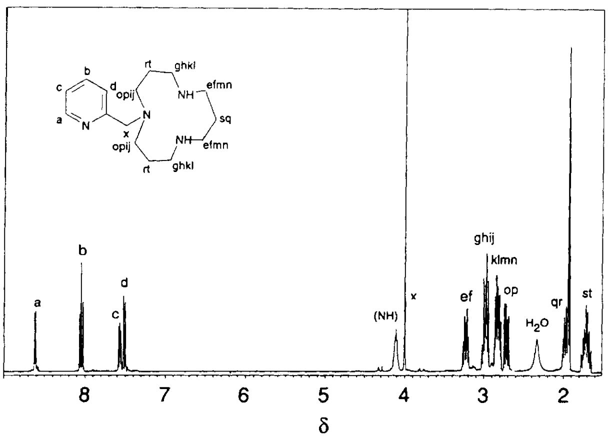

Fig. 1 Assignment of the protons of L^1 in the complex $[ZnL^1(OH_2)]^{2+}$ to NMR resonances, from a COSY NMR experiment (e = f, m = n, o = p, i = j, g = h, k = l)

However, the nickel(II) complexes of L^1 and L^2 are analogous to $[NiL^3]^{2+}$, showing irreversible oxidations to Ni^{III}.[4]

The ^1H NMR spectra of $[ZnL^1(OH_2)][NO_3]_2$ and $[ZnL^2][NO_3]_2$ in CD_3CN show very complicated splitting patterns in the aliphatic region, and assignments were made with the aid of COSY NMR spectra. The assignment for $[ZnL^1(OH_2)][NO_3]_2$ is illustrated in Fig. 1. In the ^1H NMR spectrum of $[ZnL^2][NO_3]_2$ there are two distinct sets of resonances, attributed to two geometric isomers by comparison with the ^{13}C NMR spectrum. The complicated splitting patterns in the ^1H NMR arise from the coupling of individual protons within the macrocycle, indicating that these are held in a rigid conformation around the metal cation. The ^1H NMR spectrum of $[ZnL^1(OH_2)][NO_3]_2$ in CD_3CN reveals the presence of a broad resonance at δ 2.35, which integrates for the two protons of a co-ordinated water molecule. There is prior evidence that zinc(II) complexes of triazamacrocyclic ligands containing a nitrogen donor pendant arm may adopt a tetrahedral or trigonal-bipyramidal co-ordination geometry in the solid state.[1,2,19,20] Two isomers of trigonal-bipyramidal geometry are possible as illustrated in Fig. 2. The symmetric isomer arises when the pendant arm is co-ordinated in the equatorial position, and the asymmetric isomer arises when the pendant arm is co-ordinated in the axial position. If one assumes that L^1 behaves as a tetradentate ligand, then the presence of a co-ordinated water molecule excludes the possibility of a tetrahedral co-ordination geometry in solution. It is evident from the number of resonances in the ^{13}C NMR spectrum of $[ZnL^1(OH_2)]^{2+}$ (Table 2) that this complex is the symmetric isomer of trigonal-bipyramidal co-ordination geometry (Fig. 2, structure **B**).

Two distinct sets of resonances in the ^{13}C NMR spectrum of $[ZnL^2]^{2+}$ (Table 2) indicate the existence of a *ca.* 2:1 mixture of two isomers, one symmetric (major component) and the other asymmetric. Structural studies indicate that the complex adopts a symmetric tetrahedral geometry (Fig. 2, structure **A**) as found in the solid state (Fig. 3), although in solution the possibility that the complex adopts a symmetric trigonal-bipyramidal geometry (Fig. 2, structure **B**) cannot be ruled out. The minor set of resonances is attributed to an asymmetric isomer of trigonal-bipyramidal geometry (Fig. 2, structure **C**). The presence of a co-ordinated water molecule was not detected in the ^1H NMR spectrum of this species, and we believe that the additional co-ordination site is probably occupied by a nitrate anion. Previous studies of similar zinc(II) complexes have revealed only the symmetric isomer of tetrahedral or trigonal-bipyramidal geometry.[1,2] The work of Kimura *et al.*[3] suggests that when Zn^{II} is bound to 1,5,9-triazacyclododecane, it prefers to co-ordinate an anionic donor at the equatorial position of a five-co-ordinate trigonal-bipyramidal structure containing short equatorial and long axial co-ordinate bonds, rather than exist in a four-co-ordinate tetrahedral arrangement.[3] We believe that by comparison with previously studied ligands, in solution the additional flexibility of the 2-pyridyl-2′-ethyl pendant arm of L^2 allows co-ordination of the neutral pendant arm in the axial site, thus making possible co-ordination of the nitrate anion in the equatorial site.

Crystal Structures.—To gain further insight into the structure of the zinc(II) complexes, the crystal structure of $[ZnL^2][Zn(NO_3)_{3.67}Cl_{0.33}]$ was determined (Fig. 3). The cation geometry is approximately tetrahedral (structure **A**, Fig. 2), where the macrocyclic ring forms the basal plane of the tetrahedron, and the pendant arm chelates at the apical site. Such a symmetric isomer gives a satisfactory explanation for the major component identified by the ^{13}C NMR spectrum of $[ZnL^2]^{2+}$ in acetonitrile solution. The tetradentate ligand L^2 encapsulates the zinc(II) cation, avoiding any interactions from counteranions. There is very little deviation amongst the individual Zn–N distances which average 2.00 Å. The zinc(II) cation sits above the plane of the macrocycle, where the chelate rings in the macrocyclic part of the ligand adopt the chair conformation. The pendant arm chelates in the flattened chair conformation. Although the chelating N–Zn–N angles, which average 106.0° and approach the full tetrahedral angle of 109.5° the non-chelating N(5)–Zn(1)–N(20) and N(9)–Zn(1)–N(20) angles of 111.1(3) and 120.8(3)° respectively, expand to larger values to compensate the inability of the propyl linkages of L^2 to fully subtend to the full tetrahedral angle. A distinct cleft in the cation structure is thus generated, and it is conceivable that in the presence of a smaller counteranion with ligating ability, further co-ordination might be possible to afford a five-co-ordinate species. The counteranion for this species was the unexpected tetranitratozincate(II) anion $[Zn(NO_3)_4]^{2-}$. The structure of $[ZnL^2]^{2+}$ is closer to the ideal tetrahedral geometry than that found for the zinc(II) complex of 1-(3-dimethylaminopropyl)-1,5,9-triazacyclododecane, where weak interactions between the supporting anions and the central zinc ion was noted,[2] and the distorted tetrahedral zinc(II) complex of 1-[3-(toluene-*p*-sulfonamido)propyl]-1,5,9-triazacyclododecane, where the chelating N–Zn–N angles (average 103.1°) and the non-chelating N–Zn–N angles (average 121.4°) are significantly removed from the ideal angles for tetrahedral co-ordination.[20]

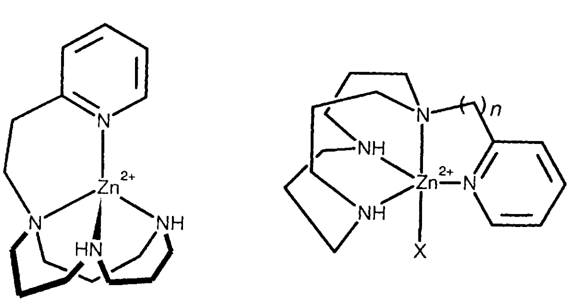

A Tetrahedral **B** Trigonal bipyramidal

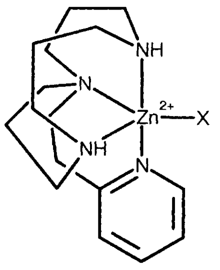

C Trigonal bipyramidal

Fig. 2 Schematic representation of isomers possible for Zn^{II} in complexes of L^1 and L^2 (X = unidentate ligand). Structures **A** and **B** are symmetric with a plane of symmetry coplanar with each pyridine ring and **C** is asymmetric

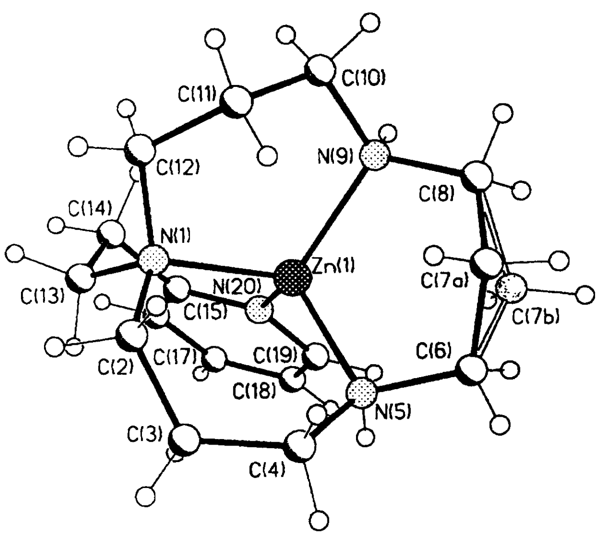

Fig. 3 X-Ray crystal structure of the $[ZnL^2]^{2+}$ cation

The crystal structure of $[NiL^1(O_2NO)]NO_3$ (Fig. 4) shows that the metal ion is pseudo-octahedral. The macrocyclic ring occupies one face of the octahedron, whilst the pendant arm chelates to a fourth site in the position *trans* to N(9) of the macrocycle. The two remaining sites are occupied by a co-ordinated bidentate nitrate ion in the position *trans* to N(1) and N(5). The Ni–O(11) and Ni–O(12) bond lengths [2.182(3) and 2.186(3) Å respectively] are typical for a chelating nitrate ion, and the Ni–N bond lengths are close to 2.08 ± 0.03 Å. Distortions from a regular octahedral geometry are evident from the N(5)–Ni–N(9) bond angle of 173.56(12)°, and the N(5)–Ni–O(11) and N(1)–Ni–O(12) bond angles of only 156.77(12) and 157.28(11)° respectively.

Conclusion

The structure determination of $[ZnL^2]^{2+}$ provides further evidence that tetrahedral co-ordination of the metal cation is more successfully achieved with a donor atom attached to a

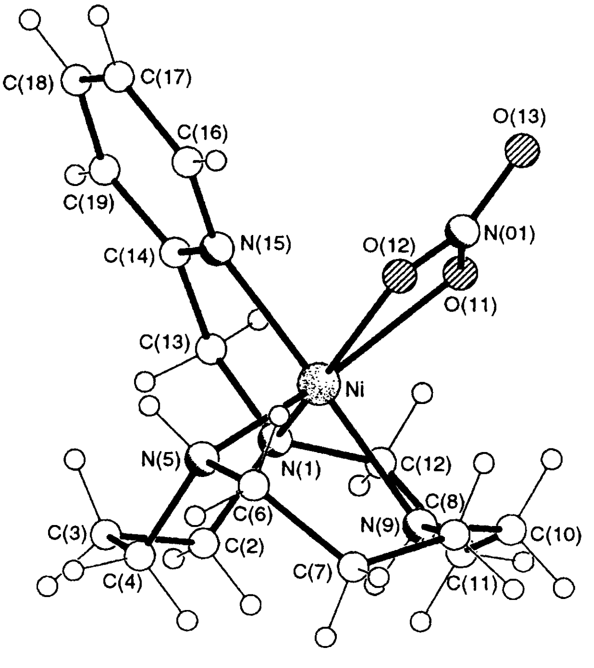

Fig. 4 X-Ray crystal structure of the $[NiL^1(O_2NO)]^+$ cation

three-carbon-linked pendant arm attached to an N atom of a twelve-membered ring triazamacrocycle. With Ni^{II} and Cu^{II}, this design is insufficient to force tetrahedral co-ordination, and it is evident that there is a fine interplay between the structural advantages of this ligand design, the reduction in complex stability as a result of the profusion of chelating propyl units, and the gain in c.f.s.e. achieved by Ni^{II} and Cu^{II} increasing their co-ordination numbers.[2] For Ni^{II} and Cu^{II}, the stability of the tetrahedral complex could possibly be enhanced by further alkylation of the remaining nitrogen donors on the macrocycle, and introduction of negatively charged pendant arms. It is towards this revised strategy that we are directing future studies.

Acknowledgements

We thank the EPSRC for financial assistance, and for provision of X-ray and mass spectrometry services at Cardiff and Swansea respectively. Dr J. Hastings and Mr P. A. Moore are thanked for their assistance with COSY NMR and CHN analyses respectively.

References

1 S. C. Rawle, A. J. Clarke, P. Moore and N. W. Alcock, *J. Chem. Soc., Dalton Trans.*, 1992, 2755.
2 N. W. Alcock, A. C. Benniston, P. Moore, G. A. Pike and S. C. Rawle, *J. Chem. Soc., Chem. Commun.*, 1991, 706.
3 E. Kimura, I. Nakamura, T. Koike, M. Shionoya, Y. Kodama, T. Ikeda and M. Shiro, *J. Am. Chem. Soc.*, 1994, **116**, 4764.
4 R. W. Alder, R. W. Mowlam, D. J. Vachon and G. R. Weisman, *J. Chem Soc., Chem. Commun.*, 1992, 507.
5 J. Cosier and A. M. Glazer, *J. Appl. Crystallogr.*, 1986, **19**, 105.
6 N. W. Alcock and P. J. Marks, *J. Appl. Crystallogr.*, 1993, **27**, 200.
7 G. M. Sheldrick, SHELTXTL PLUS user's manual, Nicolet Instrument Co., Madison, WI, 1986.
8 G. M. Sheldrick, *J. Appl. Crystallogr.*, 1994, in the press.
9 *International Tables for X-Ray Crystallography*, Kynoch Press, Birmingham, 1974, vol. 4 (present distributor Kluwer Academic Publishers, Dordrecht).
10 N. W. Alcock, F. McLaren, P. Moore, G. A. Pike and S. M. Roe, *J. Chem. Soc., Chem. Commun.*, 1989, 629.
11 S. C. Rawle, P. Moore and N. W. Alcock, *J. Chem. Soc., Chem. Commun.*, 1992, 684.
12 L. J. Zompa, *Inorg. Chem.*, 1978, **17**, 2531.
13 T. J. Riedo and T. A. Kaden, *Helv. Chim. Acta*, 1979, **62**, 1089.
14 M. Kodama and E. Kimura, *J. Chem. Soc., Dalton Trans.*, 1977, 1473.
15 M. Kodama and E. Kimura, *J. Chem. Soc., Dalton Trans.*, 1978, 104.
16 D. Zhang and D. H. Busch, *Inorg. Chem.*, 1994, **33**, 5138.
17 G. R. Weisman, D. J. Vachon, V. B. Johnson and D. A. Gronbeck, *J. Chem. Soc., Chem. Commun.*, 1987, 886.
18 A. J. Blake, I. A. Fallis, R. O. Gould, S. Parsons, S. A. Ross and M. Schroder, *J. Chem. Soc., Chem. Commun.*, 1994, 2467.
19 E. Kimura, Y. Kurogi, M. Shionoya and M. Shiro, *Inorg. Chem.*, 1991, **30**, 4524.
20 T. Koike, E. Kimura, K. Nakamura, Y. Hashimoto and M. Shiro, *J. Am. Chem. Soc.*, 1992, **114**, 7338.

Received 4th *July* 1995; *Paper* 5/04329H